JOC The Journal of Organic Chemistry

Article

pubs.acs.org/joc

Stable Nonaromatic [20]Dithiaporphyrin (2.1.1.1) Macrocycles: Synthesis, Structure, Spectral, Electrochemical, and Metal Ion Sensing Studies

Emandi Ganapathi,[†] Way-Zen Lee,*[,‡] and Mangalampalli Ravikanth*[,†]

[†]Department of Chemistry, Indian Institute of Technology Bombay, Powai, Mumbai 400 076, India

[‡]Instrumentation Center, Department of Chemistry, National Taiwan Normal University, Ting-Chow Road, Taipei, 11677, Taiwan

Supporting Information

ABSTRACT: Stable nonaromatic [20]dithiaporphyrin (2.1.1.1) macrocycles were synthesized in decent yields by condensing readily available butene-2,3-diyl-bisthiophene-2,5-diyl-bis(*p*-methoxyphenylmethanol) with different *meso*-aryl dipyrromethanes under mild acid-catalyzed conditions. The [20]dithiaporphyrin (2.1.1.1) macrocycles are the first members of the expanded porphyrin analogues of [18]-dithiaporphyrin (1.1.1.1) and consist of two pyrroles and two thiophenes connected through five *meso*-carbon bridges. The [20]dithiaporphyrin macrocycles were confirmed by mass spectroscopy, 1D and 2D NMR spectroscopy, and X-ray crystallography. The X-ray structure revealed that the macrocycle is highly distorted and that the two thiophene rings are completely out-of-plane from the "mean-plane" defined by the dipyrromethene moiety and the two *meso*-carbons. In the absorption spectrum, the macrocycles showed one strong band at ~420 nm and one weak band at ~720 nm. The electrochemical studies revealed that the macrocycles are stable under redox conditions. The metal sensing studies indicated that these macrocycles have the potential to sense specific metal ions such as Hg^{2+} ions. Two covalently linked dithiahomoporphyrin−fluorophore dyads were synthesized by coupling iodo-functionalized dithiahomoporphyrin with an ethynyl-functionalized fluorophore such as boron−dipyrromethene (BODIPY) and BF_2−smaragdyrin under mild Pd(0) coupling conditions. The potential of these dyads as a fluorescent sensor for Hg^{2+} was explored, and the studies indicated that both dyads can be used as fluorescent sensors.

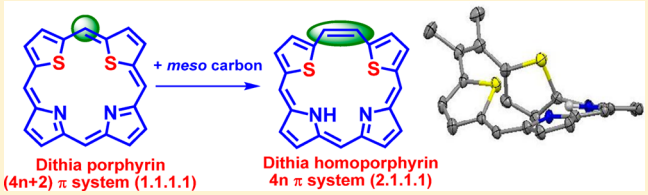

INTRODUCTION

Porphyrins are 18π aromatic macrocycles consisting of four pyrroles that are connected in a coplanar fashion at their α-carbon atoms through four methine carbon bridges.[1] The simplest higher homologue of 18π porphyrin (1.1.1.1) is the 20π expanded porphyrin macrocycle[2] which contains an extra methine carbon between one of the methine carbons and an α-pyrrolic carbon. Thus, the 20π expanded porphyrin consists of four pyrroles connected through five methine bridges and can be represented as [20]porphyrin (2.1.1.1). A perusal of the literature indicated that such 20π systems with five *meso*-carbon bridges are called homoporphyrins[2a,3] which were synthesized by chemical and electrochemical approaches using metalloporphyrins as precursors. The homoporphyrins synthesized by Grigg[3] and Callot and co-workers[4] during 1967−1979 were found to be extremely unstable and decomposed even at 0 °C. The instability of the homoporphyrins was attributed to their nonaromatic nature. It is common notion that the 4nπ porphyrinoid macrocycles[5] are generally unstable. However, recently several 4nπ-based stable expanded porphyrinoids[6] with 24π, 28π, 32π, 36π, 40π, 48π, and 64π electrons were synthesized and structurally characterized.

Interestingly, no proper synthetic strategy has been developed to obtain stable 20π expanded porphyrin macrocycles (2.1.1.1), which are the first member of the expanded porphyrin macrocycles. Very recently, Shen and co-workers reported[7] a stable 20π-electron porphyrin system (1.1.1.1) by introducing a fused thienopyrrole moiety which stabilized the nonaromatic macrocycle. This indicates that the presence of heterocycles such as thiophene in the place of pyrrole would stabilize the 20π electron macrocycle. Thus, 18π 21,22-dithiaporphyrin,[8] a (4n+2)π aromatic system, can be converted to the stable 20π nonaromatic (4n)π dithiahomoporphyrin system by introducing one additional methine carbon between the two thiophene rings that are linked by one methine carbon using properly designed precursors (Chart 1). Herein, we used two readily available precursors, butene-2,3-diyl-bisthiophene-2,5-diyl-bis(*p*-methoxyphenylmethanol) **11** and *meso*-aryl dipyrromethane,[9] to synthesize the first stable [20]-dithiaporphyrin (2.1.1.1) macrocycles **1**−**4** under mild acid-catalyzed conditions at room temperature (Scheme 1). These dithiahomoporphyrin macrocycles **1**−**4** containing two thiophenes and two pyrroles connected via five methine carbon atoms exhibited interesting spectral and redox properties. The crystal structure showed that the macrocycle is highly distorted.

Received: July 29, 2014
Published: September 12, 2014

dx.doi.org/10.1021/jo501724d | J. Org. Chem. 2014, 79, 9603−9612

Chart 1

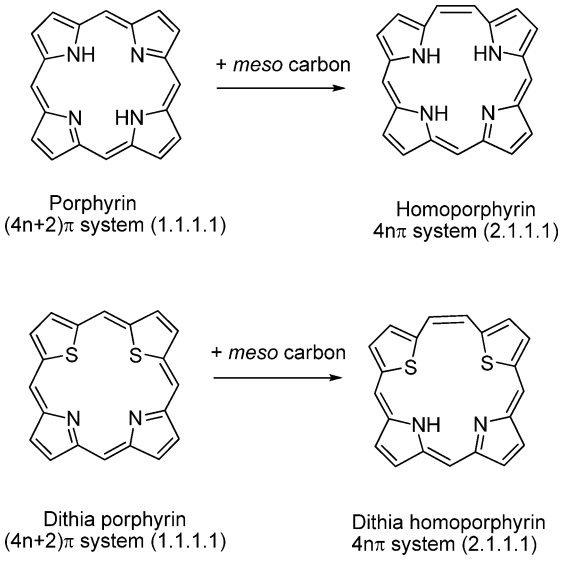

These dithiahomoporphyrins showed specificity toward Hg(II) ion as confirmed by optical, NMR, and mass studies. To show further use of dithiahomoporphyrins, we synthesized covalently linked dithiahomoporphyrin–boron dipyrromethene (BODIPY) dyad **5** and dithiahomoporphyrin–BF_2–smaragdyrin dyad **6** and demonstrated that dithiahomoporphyrin–BODIPY dyad **5** can be used as a fluorescent turn-on sensor for Hg(II) ion.

RESULTS AND DISCUSSION

The desired diol **11** was synthesized in two steps starting with 2-acetylthiophene **13**. McMurry coupling of 2-acetylthiophene **13** afforded a mixture of *E*- and *Z*-isomers of 2,3-dithianyl-2-butene[10] **12** which was, upon subsequent reaction with *n*-BuLi, followed by addition of 4-methoxybenzaldehyde in THF to give diol **11** as a white solid in 65% yield. The [20]dithiaporphyrin (2.1.1.1) macrocycles **1**–**4** were prepared by [2 + 2] condensation of 1 equiv of diol **11** with 1 equiv of appropriate *meso*-aryl dipyrromethane **7**–**10** in CH_2Cl_2 in the presence of 1 equiv of TFA for 1 h under N_2 atmosphere followed by oxidation with DDQ for an additional 1 h in open air. TLC analysis showed only one nonfluorescent green spot corresponding to the desired macrocycle, indicating that the condensation was very straightforward with exclusive formation of the desired macrocycle. The crude reaction mixtures were subjected to alumina column chromatography and afforded macrocycles **1**–**4** as green solids in 15–20% yields (Scheme 1). The macrocycles **1**–**4** were freely soluble in common organic solvents and characterized by mass, spectral and electrochemical techniques, and by X-ray crystallography for macrocycles **1** and **3**. High-resolution mass spectrometry confirmed the composition of [20]dithiaporphyrin (2.1.1.1) macrocycles **1**–**4**.

NMR Studies. The structures of macrocycles **1**–**4** were clearly deduced by 1D and 2D NMR studies. The ^{1}H NMR spectra of macrocycles **1** and **4** are shown in Figure 1a, and the key regions of the NOESY spectra of macrocycles **1** and **4** are

Scheme 1. Synthesis of Homoporphyrins 1–4

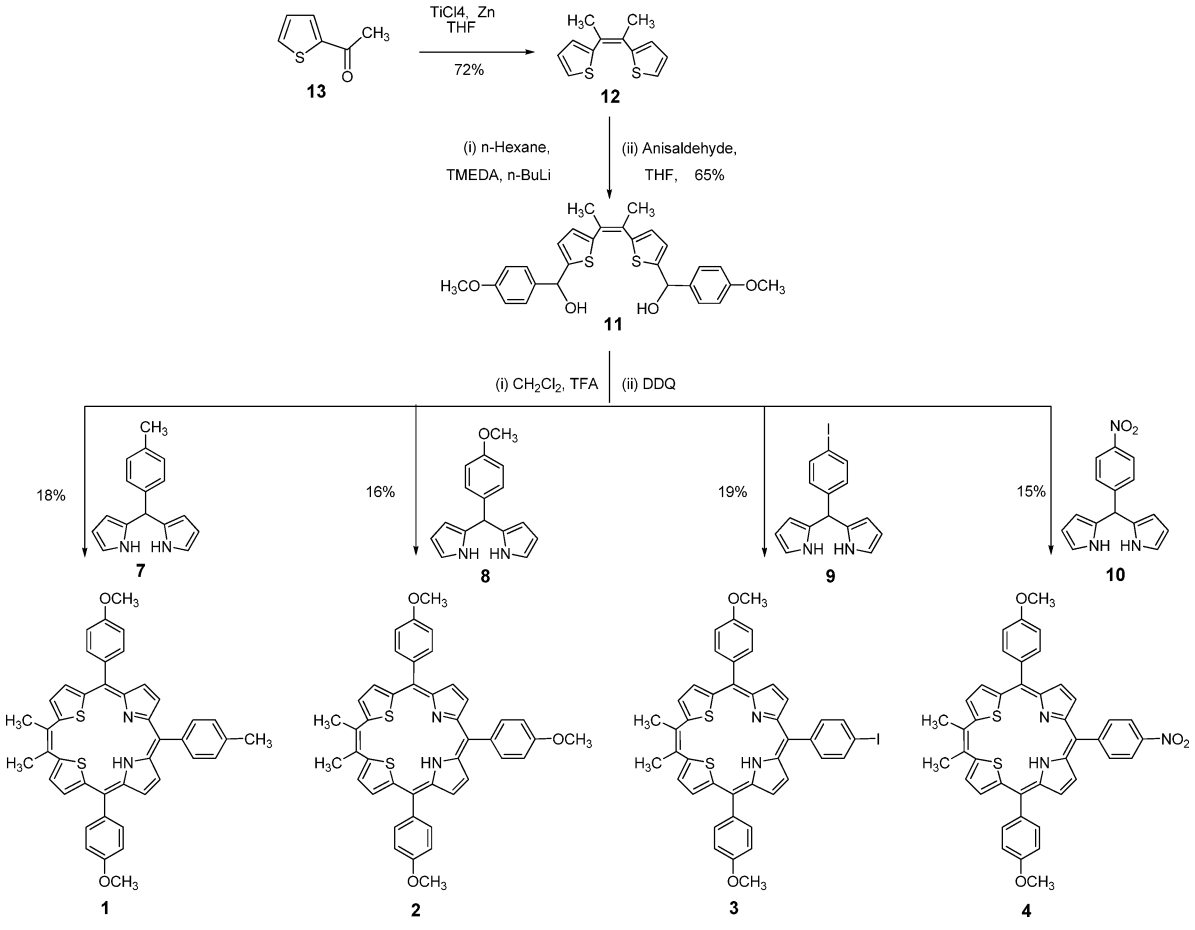

dx.doi.org/10.1021/jo501724d | J. Org. Chem. 2014, 79, 9603–9612

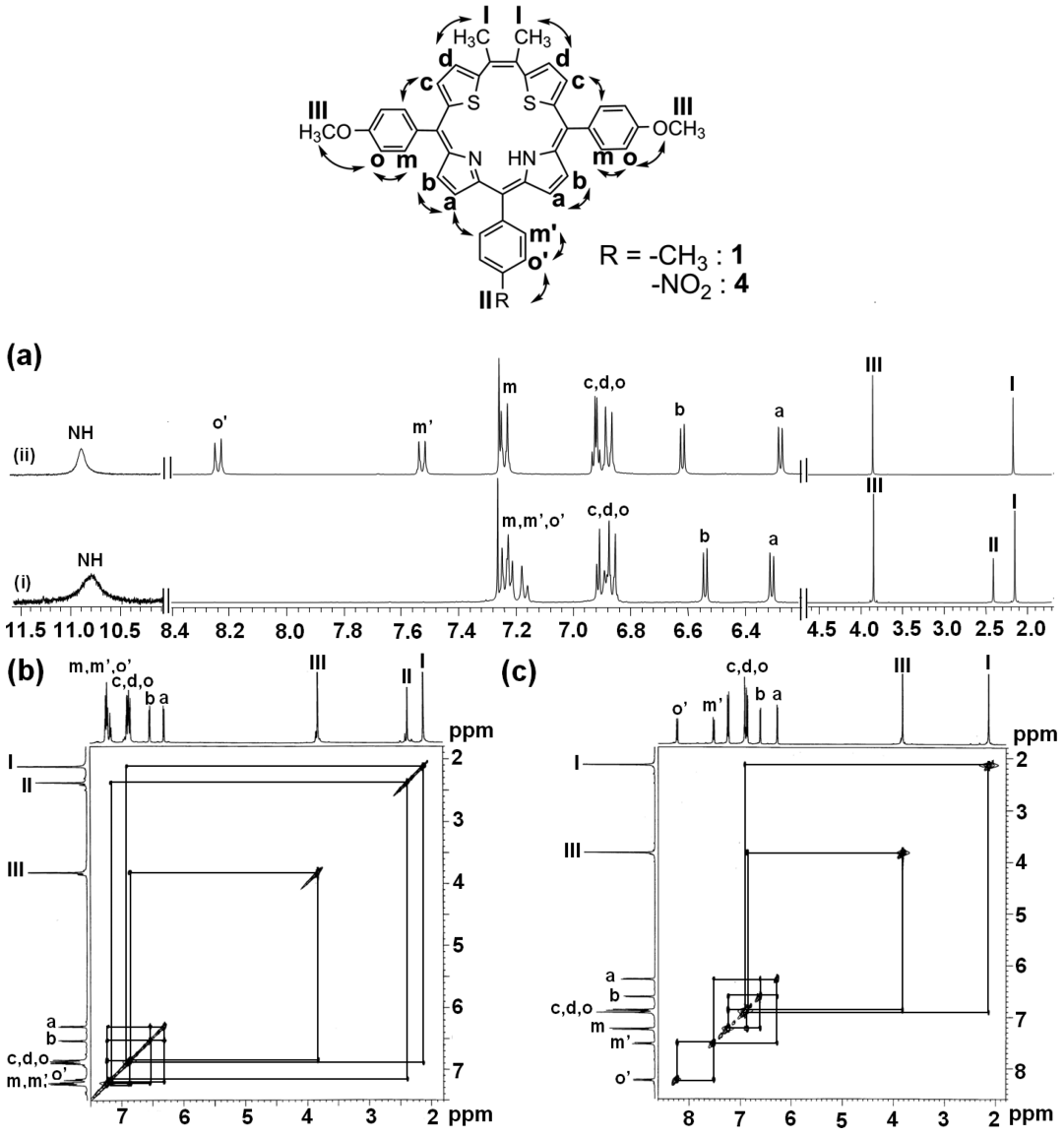

Figure 1. (a) Comparison of ^{1}H NMR spectra of macrocycles (i) **1** and (ii) **4**. (b) NOESY spectrum of **1** and (c) NOESY spectrum of **4** showing NOE connectivities.

shown in Figure 1b and 1c, respectively. The ^{1}H NMR spectrum of macrocycle **1** showed the following features: three singlets at 2.12, 2.38, and 3.82 ppm corresponding to six methyl protons present on the ethylene bridge (type I), three methyl protons of the *meso*-tolyl group (type II), and six methoxy protons of *meso*-anisyl group (type III), respectively; two doublets at 6.31 and 6.53 ppm corresponding to two protons each and two clusters of signals corresponding to eight protons each in 6.86−6.91 ppm and 7.16−7.24 ppm regions. The assignments of all resonances were made using cross-peak correlations in COSY and NOESY spectra and coupling constants in the ^{1}H NMR spectrum. In the ^{1}H−^{1}H COSY spectrum, the two doublets at 6.31 and 6.53 ppm showed cross-peak correlation (Supporting Information (SI)) with a coupling constant of ∼5 Hz, indicating that these two doublets are from five-membered heterocycles such as pyrrole or thiophene but not from the *meso*-aryl protons. Furthermore, close inspection of the cluster in the region of 7.16−7.24 ppm showed three very close sets of doublets at 7.16, 7.21, and 7.23 ppm with a coupling constant of ∼7 Hz corresponding to four, two, and two protons, respectively, and the doublets at 7.16 and 7.21 ppm showed cross-peak correlation in the ^{1}H−^{1}H COSY spectrum (SI). Similarly, the cluster in the region of 6.86−6.91 ppm also showed the presence of one doublet at 6.86 ppm for four protons with a coupling constant of ∼7 Hz and one multiplet for four protons at 6.88 ppm. Thus, the doublets present in these two clusters are from *meso*-aryl groups and the multiplet at 6.88 ppm is due to the heterocyclic ring. At this stage, we focused our attention on the NOESY spectrum to identify and assign all *meso*-aryl and heterocyclic resonances in ^{1}H NMR of macrocycle **1**. In the NOESY spectrum of **1**, the methoxy protons of the anisyl group appeared as a singlet at 3.82 ppm (type III) and showed NOE correlation (Figure 1b) with a doublet at 6.86 ppm that appeared in the cluster of signals in 6.86−6.91 ppm region which we assigned to type o protons of the *meso*-anisyl group. The type o protons showed correlation with the doublet at 7.23 ppm in the COSY spectrum which was assigned as type m protons of the *meso*-anisyl group. At the same time, the methyl resonance of the ethylene bridge appearing as a singlet at 2.12 ppm (type I) also

dx.doi.org/10.1021/jo501724d | J. Org. Chem. 2014, 79, 9603−9612

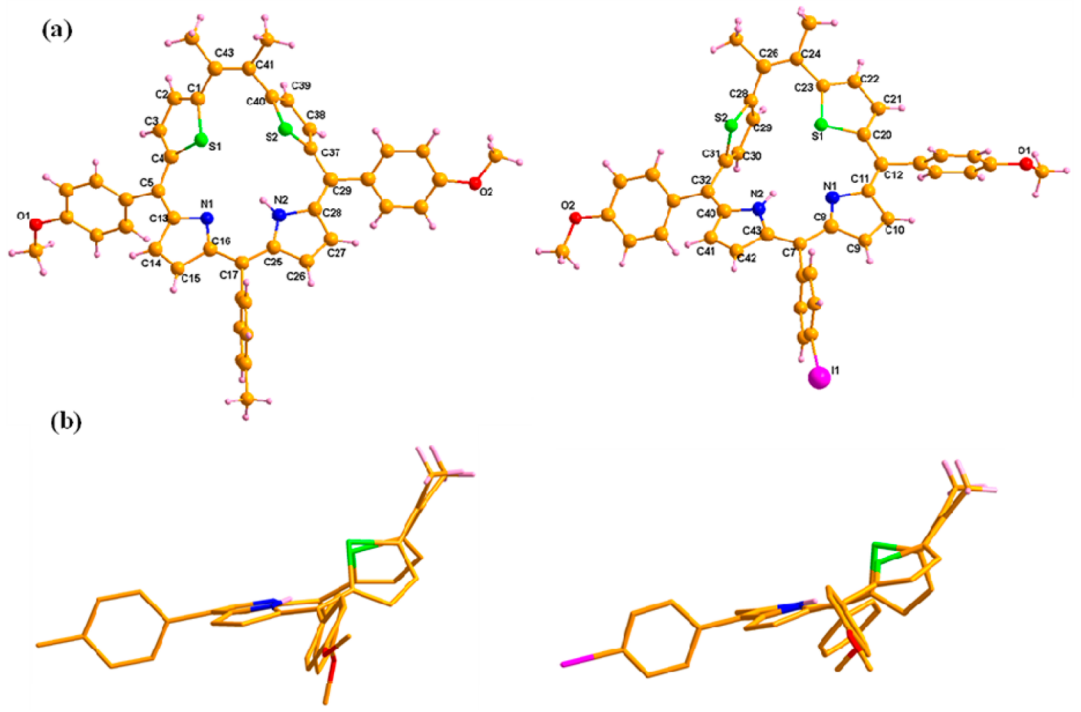

Figure 2. Single crystal X-ray structures of macrocycles **1** and **3**: (a) perspective view, and (b) side view showing the chairlike arrangement of the macrocycles. Some of the hydrogens are omitted for clarity.

showed NOE correlation with the multiplet at 6.88 ppm (Figure 1b) which was assigned to four thiophene protons of type c and d. The type c and d thiophene protons did not show NOE correlation with any other resonances except with the methyl resonance because the thiophene rings are oriented away from the other protons (vide infra). The methyl resonance of tolyl appearing as a singlet at 2.38 ppm (type II) showed NOE correlation with the doublet at 7.16 ppm corresponding to two protons that were identified as type o′ protons which in turn showed cross-peak correlation with doublet at 7.21 ppm in the ^{1}H−^{1}H COSY spectrum which was assigned to type m′ protons of the *meso*-tolyl group. The type m protons that appeared as a doublet at 7.23 ppm showed NOE correlations with the doublet at 6.53 ppm which was assigned to type b pyrrole protons (Figure 1b and Supporting Information). The doublet at 6.53 ppm (type b) showed cross-peak correlation with the doublet at 6.30 ppm which in turn showed NOE correlation with type m′ protons at 7.21 ppm and was assigned to type a pyrrole protons. To further confirm the assignments for all resonances, we carried out 1D and 2D NMR studies on macrocycle **4** which contains a 4-nitrophenyl group on the *meso*-dipyrromethene unit of the macrocycle in place of the *meso*-tolyl group of macrocycle **1**. The ^{1}H NMR spectrum of macrocycle **4** showed NMR features similar to those observed for macrocycle **1** except for the three close doublets appearing in the 7.16−7.24 ppm region of macrocycle **1** which were well separated in macrocycle **4** and appeared as three clear sets of doublets at 7.24, 7.53, and 8.24 ppm corresponding to four, two, and two protons, respectively. On the basis of 2D NMR studies, we identified all the *meso*-aryl, pyrrole, and thiophene protons (Figure 1a(ii), Figure 1c). The two other macrocycles, **2** and **3**, showed NMR features similar to those observed for macrocycles **1** and **4**. The inner NH proton was observed at ∼11 ppm in macrocycles **1**−**4**. Thus, the upfield shifts of heterocycle proton resonances and the downfield shift of the inner NH proton resonance unambiguously confirms the nonaromatic nature[5] of the macrocycles **1**−**4**.

Crystallographic Characterization. The conclusive proof for the formation of stable [20]dithiaporphyrin (2.1.1.1) macrocycles was unambiguously confirmed by single crystal X-ray structures obtained for macrocycles **1** and **3**. The macrocycles **1** and **3** were crystallized by slow diffusion of *n*-hexane into CH_2Cl_2 solution (CCDC-923462 and 1005187). Macrocycles **1** and **3** were crystallized in triclinic space group *P*1; the ORTEP plots of macrocycles **1** and **3** are presented in Figure 2, and the relevant crystallographic data are presented in Table 1. Figure 2clearly shows that the macrocycles are highly distorted and that the two thiophene rings are completely out-of-plane from the "mean-plane" defined by the dipyrromethene moiety and the two *meso*-carbons (C5 and C29 in macrocycle **1** and C12 and C32 in macrocycle **3**). Because of the larger size of the sulfur, the macrocycles adopted chairlike structures (Figure 2b), with the dithiophene ethylene moiety positioned above the mean-plane to release the strain of the macrocycles. The two sulfur atoms deviate from the mean plane (1.624 Å, 2.072 Å in macrocycle **1** and 1.233 Å, 1.903 Å in macrocycle **2**). Similarly, the two *meso*-carbons (∼2.90 Å in macrocycle **1** and 2.45 Å in macrocycle **2**) of the ethylene bridge also largely deviate from the mean plane. The two pyrrole "N"s (0.185 Å for N1 and 0.122 Å for N2 in macrocycle **1** and 0.099 Å for N1 and 0.191 Å for N2 in macrocycle **2**) also showed slight deviation from the mean plane. Because the thiophene sulfurs largely deviate from the mean plane, the distance between diagonal thiophene "S" and pyrrole "N" is longer than expected (Table 2). The dihedral angles between mean plane and the *meso*-anisyls which are *trans* to each other (56° and 70° in macrocycle **1** and 36° and 65° in macrocycle **2**) are much smaller than the dihedral angle of the *meso*-tolyl/iodo group (∼80°). The dihedral angles between the mean plane and the thiophene (S1, S2)-containing planes are 40°, 65° in macro-

dx.doi.org/10.1021/jo501724d | *J. Org. Chem.* 2014, 79, 9603−9612

Table 1. Crystallographic Data for Macrocycles 1 and 3

parameters	1	3
CCDC no.	923462	1005187
mol formula	$C_{44}H_{36}N_2O_2S_2$	$C_{43}H_{33}IN_2O_2S_2$
fw	688.87	800.73
cryst sym	triclinic	triclinic
space group	*P*1	*P*1
a (Å)	11.094(4)	9.779(5)
b (Å)	12.716(4)	15.510(9)
c (Å)	13.616(5)	15.774(8)
α (deg)	72.135(5)	115.884(10)
β (deg)	74.147(6)	104.725(9)
γ (deg)	82.734(6)	90.077(10)
V (Å^3)	1756.8(11)	2064.3(18)
Z	2	2
μ (mm^{-1})	0.193	0.912
D_{calcd} (mg m^{-3})	1.302	1.288
F(000)	724	812
2θ range (deg)	1.62 to 25.01	1.45 to 25.27
e data (R_{int})	6134 [*R*(int) = 0.0734]	7382 [*R*(int) = 0.0892]
R1, wR2 [$I > 2\sigma(I)$]	R1 = 0.0660, wR2 = 0.1546	R1 = 0.0986, wR2 = 0.2239
R1, wR2 (all data)	R1 = 0.1486, wR2 = 0.2058	R1 = 0.2586, wR2 = 0.3150
GOF	1.000	1.314
largest diff peak/hole (e Å^{-3})	0.208/−0.278	1.564/−0.799

Table 2. Selected Bond Lengths (Å) and Bond Angles (deg) for Macrocycles 1 and 3

	1	3
Bond Lengths (Å)		
S1−S2	3.39	3.51
N1−N2	2.83	2.92
S1−N1	3.04	3.03
S2−N2	3.34	3.49
S1−N2	4.23	4.17
S2−N1	4.64	4.92
N2−H2···N1	2.28	2.38
Bond Angles (deg)		
125.3, 128.3	C4−C5−C13	C11−C12−C20
121.7, 118.25	C28−C29−C37	C31−C32−C40
124.5, 124.8	C16−C17−C25	C43−C7−C8

cycle **1** and 29°, 80° in macrocycle **2**. An intramolecular hydrogen-bonding interaction in the core between N2−H2···N1 (H2−N1 2.28 Å in macrocycle **1** and 2.38 Å in macrocycle **2**) is also noted. In the crystal packing, the weak intermolecular hydrogen bonding interactions between *meso*-methyls of one macrocycle and the pyrrole nitrogen of another macrocycle and also between the methoxy oxygen of one macrocycle and the aryl hydrogen of another macrocycle leads to a three-dimensional supramolecular architechture (Figure S47 in SI). Thus, the crystal structures indicated that the presence of additional *meso*-carbon and the unique orientation of the thiophene rings assisted in the stability of the macrocycles. The nonaromatic character of these macrocycles were obtained by computing the nucleus-independent chemical shift (NICS)[11] values by employing Gaussian 03.[12] The computed NICS(0) values for the two homoporphyrin systems **1** and **3** were found to be δ = 0−2 ppm (Tables S1 and S2 in SI). The ^{1}H NMR signals of macrocycles **1**−**4** in $CDCl_3$ for β-protons are located in the 6−7 ppm region, and the NICS values are 0 to 2.0 ppm at several points around the macrocycles **1** and **3** (Tables S1 and S2 in SI). On the basis of these data, macrocycles **1**−**4** have been regarded as nonaromatic species.[5]

Absorption and Electrochemical Studies. The absorption spectra of macrocycles **1**−**4** and their protonated derivatives **1**.H$^+$−**4**.H$^+$ were recorded in dichloromethane, and the data are presented in Table 3. The comparison of absorption spectra of **1** and its protonated derivative **1**.H$^+$ is shown in Figure 3a. Figure 3 clearly shows that macrocycle **1** exhibits one moderately strong absorption band at ∼410 nm and a low intensity broad absorption band at ∼720 nm (Figure 3). The other three macrocycles **2**−**4** also showed similar absorption spectra with slight shifts in their absorption peak maxima (Figures S30−S32 in SI). These absorption features are in agreement with the typical features exhibited by non/antiaromatic macrocyclic systems.[5] Upon protonation, the color of the solution changed from green to yellow and the absorption bands experienced bathochromic shifts and appeared at ∼424 nm and ∼840 nm (Figure 3a).

Table 3. Absorption Data for Macrocycles 1−4 and Their Protonated Forms 1.H$^+$−4.H$^+$

compound no.	$\lambda_{(abs)}$ (nm) (log ε)	
1	412 (5.20)	720 (4.90)
1.H$^+$	422 (5.17)	844 (5.04)
2	410 (5.36)	724 (4.83)
2.H$^+$	418 (5.29)	848 (5.01)
3	412 (5.26)	722 (4.86)
3.H$^+$	424 (5.19)	840 (5.02)
4	406 (5.17)	716 (4.94)
4.H$^+$	436 (5.15)	834 (5.08)

The redox properties of macrocycles **1**−**4** were studied by cyclic voltammetry (CV) and differential pulse voltammetry (DPV) at a scan rate of 50 mV/s using tetrabutylammonium perchlorate as supporting electrolyte (0.1 M) in dichlomethane. The representative cyclic voltammogram along with DPV for macrocycle **1** is shown in Figure 3b, and the data for all compounds are given in Table 4. Macrocycles **1**−**4** showed two reversible oxidations and two reversible/quasireversible reductions. For example, macrocycle **1** showed two reversible oxidations at 0.37 and 0.68 V and two quasireversible reductions at −1.15 and −1.55 V (Figure 3b). The other three macrocycles **2**−**4** also showed similar redox behavior with slight changes in their redox potentials, depending on their *meso*-aryl groups (Figures S37−S39 in SI). Thus, electrochemical study indicated that the dithiahomoporphyrins **1**−**4** are very stable under redox conditions. Furthermore, the photophysical studies indicated that the macrocycles **1**−**4** are nonfluorescent.

Metal Ion Sensing Studies. These studies were carried out to understand the potential of these 20π dithiaporphyrin (2.1.1.1) macrocycles toward sensing various metal ions. Among various metal chlorides (Na^+, K^+, Ca^{2+}, Mg^{2+}, Mn^{2+}, Fe^{2+}, Co^{2+}, Ni^{2+}, Zn^{2+}, Cd^{2+}, Pb^{2+}, Hg^{2+}, Cu^{2+}) which were added to a solution of macrocycle **1** in CH_2Cl_2, the addition of Hg^{2+} ion resulted in instant color change from green to yellow which was accompanied by clear shifts in absorption bands (Figures S42 and S43 in SI). Thus, we carried out absorption spectral titration of macrocycle **1** with increasing amounts of Hg^{2+} in CH_2Cl_2 as shown in Figure 4. The addition of Hg^{2+}

dx.doi.org/10.1021/jo501724d | J. Org. Chem. 2014, 79, 9603−9612

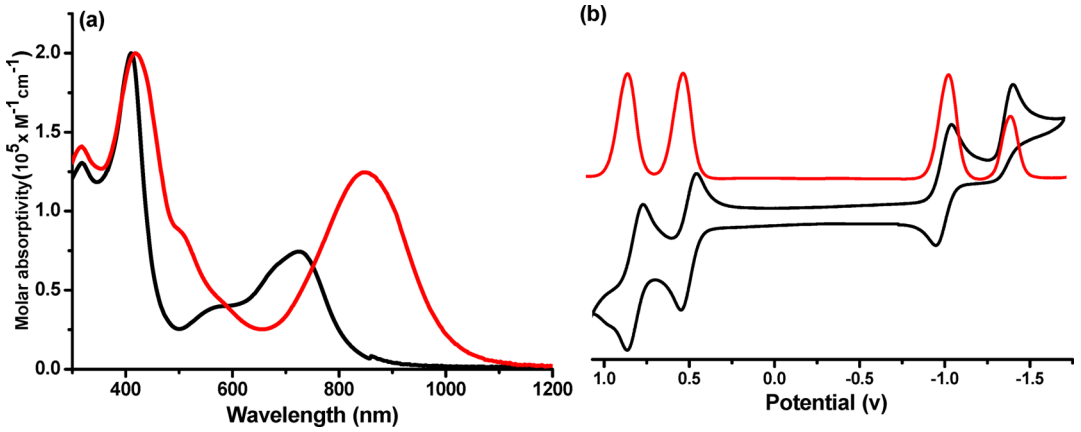

Figure 3. Comparison of (a) absorption spectra of macrocycle **1** (black line) and its protonated macrocycle **1**.H^+ (red line). (b) Cyclic voltammogram (black line) and differential pulse voltammogram (red line) of macrocycle **1**.

Table 4. Redox Data for the Macrocycles 1−4 Obtained in Dichloromethane Containing 0.1 M TBAP as Supporting Electrolyte Recorded at 50 mV s^{-1} Scan Rate

	oxidation $E_{1/2}$/V vs SCE		reduction $E_{1/2}$/V vs SCE	
compound no.	I	II	I	II
1	0.37	0.68	−1.14	−1.55
2	0.35	0.66	−1.11	−1.54
3	0.41	0.70	−1.11	−1.52
4	0.46	0.71	−1.12	−1.58

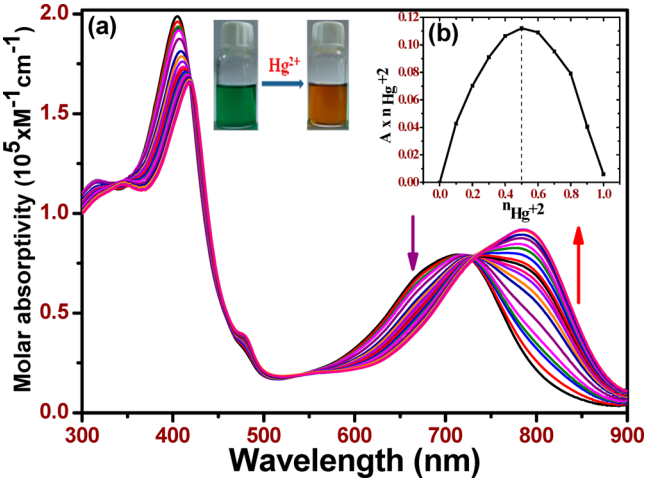

Figure 4. (a) Absorption spectral change of macrocycle **1** (5×10^{-5} M) upon addition of increasing equivalents of Hg^{2+} ions (0−2 equiv) in CH_2Cl_2 solution. (The inset shows the color change of macrocycle **1**). (b) Job's plot for the evolution of binding stiochiometry between macrocycle **1** and Hg^{2+} in CH_2Cl_2 where $n_{Hg^{2+}}$ is the mole fraction of Hg^{2+} ion added and *A* is the absorbance of compound **1** in the presence of Hg^{2+} which forms a 1:1 complex in the corresponding inset.

ions (0−2 equiv) to a CH_2Cl_2 solution of **1** resulted in a bathochromic shift of absorption bands from 412 and 720 nm to 422 and 786 nm, respectively, with a clear isosbestic point at 731 nm. However, the presence of other metal ions did not change the color of the solution, and no shifts were noted in the absorption peak maxima. To determine the binding stoichiometry, we carried out absorption titration experiments in the presence of varying mole-fractions of Hg^{2+} in CH_2Cl_2 (Figure 4 inset). Job's plot analysis of changes in the absorbance reveal a maximum of ∼0.5, indicative of the formation of a 1:1 complex between macrocycle **1** and Hg^{2+} which is in agreement with the mass spectrum obtained for **1**-Hg^{2+} complex (Figure S44 in SI). From the changes in absorption spectra, the binding constant for sensing Hg^{2+} was estimated to be 5.89×10^4 M^{-1} using the Benesi−Hildebrand equation. The formation of **1**-Hg^{2+} was confirmed further by ^{1}H NMR. Upon addition of Hg^{2+} ion to macrocycle **1**, the resonances corresponding to various protons of macrocycle **1** were broadened with slight shifts, and the inner NH proton which was observed at 10.80 ppm in **1** completely disappeared upon addition of Hg^{2+} ions, supporting the formation of **1**-Hg^{2+} complex (Figure S45 in SI). Thus, the studies clearly showed that the dithiahomoporphyrins have very good potential for sensing Hg^{2+} ions in solution. However, the **1**-Hg^{2+} complex is stable only in solution, and our attempts to isolate **1**-Hg^{2+}complex failed. Further efforts will be in the direction of synthesis and isolation of metal complexes of dithiahomoporphyrins.

Covalently Linked Dyads. To establish the specific Hg^{2+} ion sensing ability of dithiahomoporphyrin macrocycles **1**−**4**, we designed covalently linked dyads in which the dithiahomoporphyrin macrocycle which is nonfluorescent is connected to fluorophores such as boron−dipyrromethene (BODIPY) and BF_2−smaragdyrin. These dyads were synthesized with an idea that the Hg^{2+} ion binding at the nonfluorescent homoporphyrin site can be monitored by following the changes in the fluorescence of the fluorophore unit; thus, dyads could be used as fluorescent sensors for Hg^{2+} ion. The covalently linked dithiahomoporphyrin−BODIPY dyad **5** and dithiahomoporphyrin−BF_2−smaragdyrin dyad **6** were synthesized[13] by coupling macrocyle **3** with *meso*-ethynyl BODIPY **14** and BF_2−smaragdyrin **15**, respectively, in toluene/triethylamine in the presence of catalytic amounts of $AsPh_3$ and $Pd_2(dba)_3$ at 40 °C for 5 h followed by column chromatographic purification to afford **5** and **6** in 60−61% yields. The molecular ion peak in HR-MS confirmed the identity of the dyads **5** and **6**. The ^{1}H NMR spectrum of dyads **5** and **6** showed features that are a combination of both constituent monomers with almost no changes in the chemical shifts of various protons compared to their corresponding monomers, indicating that the two constituent units in dyads **5** and **6** interact very weakly and retain their individual characteristic features. The absorption spectra of dyads **5** and **6** recorded are essentially a linear combination of the spectra of their corresponding monomers.

dx.doi.org/10.1021/jo501724d | J. Org. Chem. 2014, 79, 9603−9612

Scheme 2. Synthesis of Covalently Linked Dyads 5 and 6

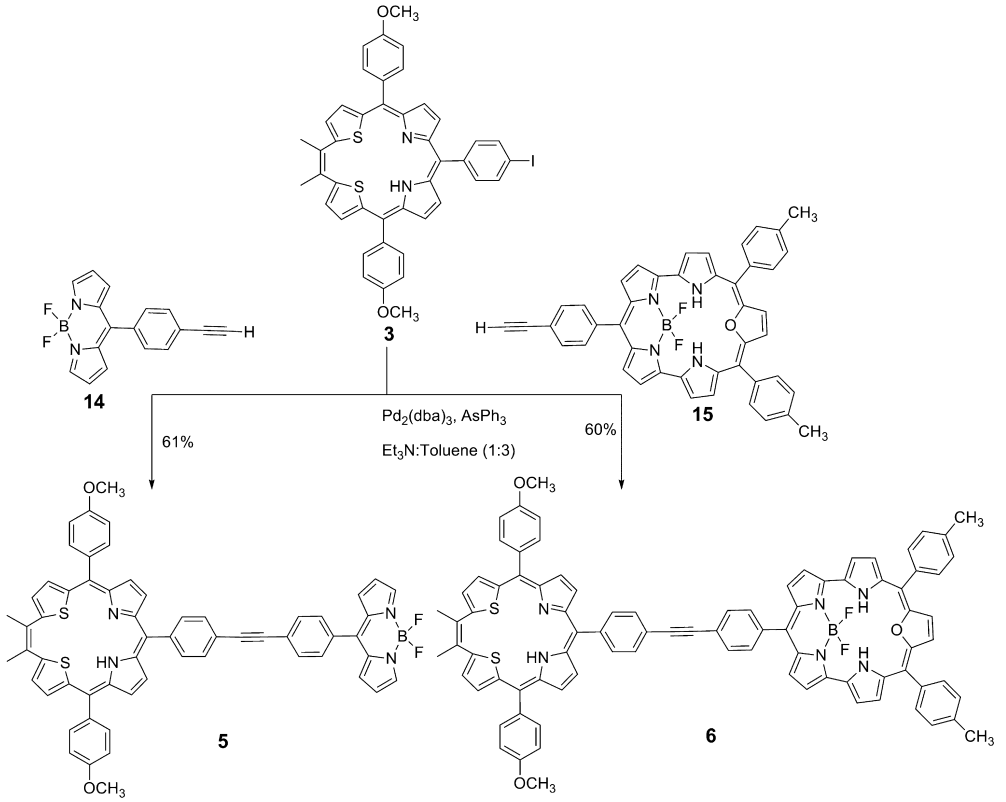

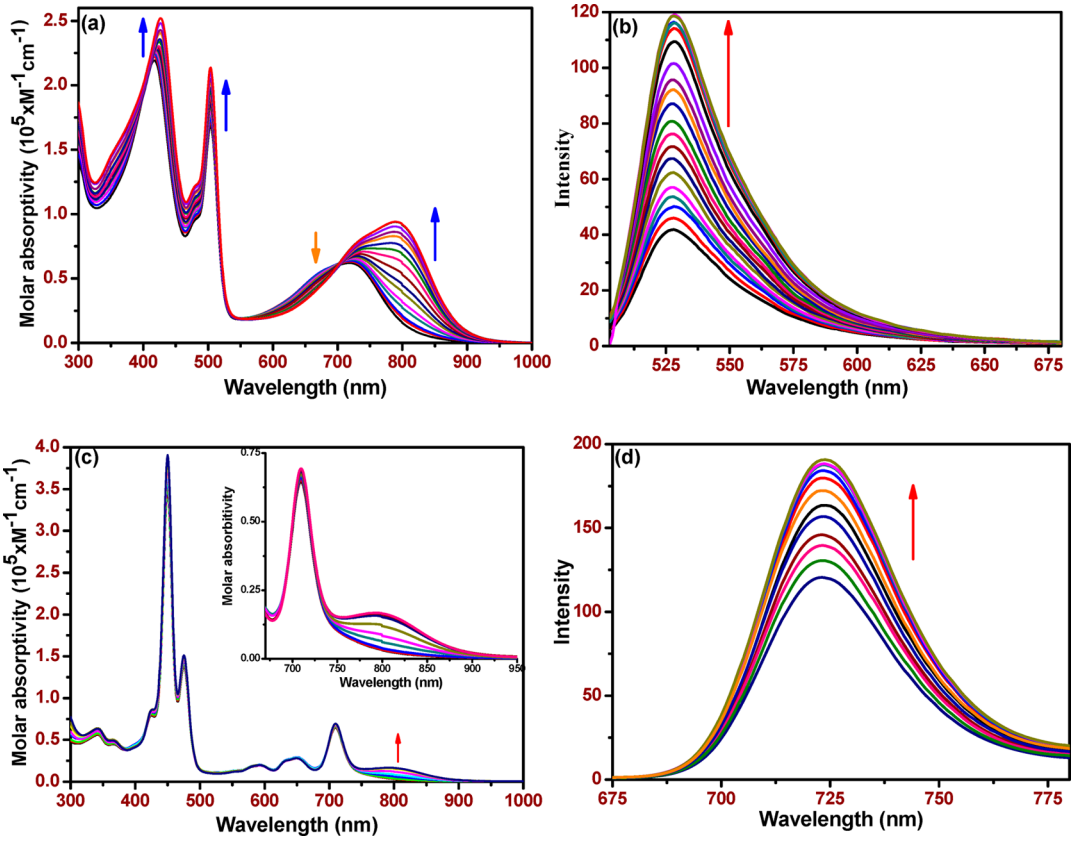

Figure 5. Absorption (a and c) and emission (b and d) spectral changes of macrocycles **5** and **6**, respectively (5×10^{-5} M), upon addition of increasing equivalents of Hg^{2+} (0–2 equiv) ions in CH_2Cl_2 solution.

dx.doi.org/10.1021/jo501724d | J. Org. Chem. 2014, 79, 9603–9612

For example, dyad **5** shows three bands at 416, 503, and 725 nm. In this spectrum, the bands at 416 and 725 nm are exclusively due to the dithiahomoporphyrin unit and the band at 503 nm is due to the BODIPY unit. However, the absorption spectrum of dyad **6** showed the absorption features dominated by the BF_2−smaragdyrin unit because the BF_2−smaragdyrin bands are much higher in intensity and the homoporphyrin absorption bands appear as shoulder bands.

The steady-state fluorescence properties of the dyads **5** and **6** were investigated by exciting the fluorophore unit, such as the BODIPY unit in dyad **5** and BF_2−smaragdyrin unit in dyad **6**, at their respective peak maxima. Dyad **5** on excitation at 488 nm, at which the BODIPY unit absorbs strongly, exhibits a fluorescence band at 527 nm with a quantum yield of 0.04. Similarly, dyad **6** on excitation at 450 nm, at which BF_2−smaragdyrin absorbs strongly, exhibits an emission band at 723 nm with a quantum yield of 0.0018. However, the respective fluorophore units in dyads **5** and **6** exhibit weak emission compared to their corresponding monomers due to electron/energy transfer from the fluorophore unit to the dithiahomoporphyrin unit. Dyads **5** and **6** along with their corresponding monomers were studied by cyclic voltammetry and by differential pulse voltammetry (DPV) in CH_2Cl_2. Dyads **5** and **6** exhibit features of both constituent monomers, and the redox potentials of dyads **5** and **6** fall in the same range as those of their constituent monomers (Figures S40 and S41 in SI). For example, dyad **5** containing BODIPY and dithiahomoporphyrin units exhibits two reversible oxidations at 0.56 and 0.85 V and three reversible/quasireversible reductions at −0.56, −0.97, and −1.40 V. Of these, both oxidations and the two reductions at −0.97 and −1.40 V were due to the dithiahomoporphyrin unit whereas the reduction at −0.56 V was exclusively due to the BODIPY unit. Dyad **6** also shows similar features, and its redox potentials are in the same range as those of its corresponding monomers (Table S4 in SI). Thus, the electrochemical study indicates that the constituent units in dyads **5** and **6** interact very weakly with each other.

To show that dyads **5** and **6** can be used for sensing Hg^{2+}, we carried out absorption and fluorescence titration experiments by adding increasing amounts of Hg^{2+} to dyads **5** and **6**, and the effects of titration of different amounts of Hg^{2+} on the absorption and fluorescence spectra of dyads **5** and **6** are shown in Figure 5. Figure 5a,c clearly shows that the addition of increasing amounts of Hg^{2+} to dyads **5** and **6** resulted in a shift of the absorption band from 720 nm to ∼790 nm with clear isosbestic points and no significant change in the absorption band(s) of the fluorophore unit, suggesting that Hg^{2+} ion binds to the dithiahomoporphyrin site in dyads **5** and **6**. The binding of Hg^{2+} to dyads **5** and **6** was also confirmed by mass analysis. Furthermore, the fluorescence spectral titrations shown in Figure 5b and 5d for dyads **5** and **6**, respectively, indicate that dyads **5** and **6** can be used as fluorescent sensors. Upon addition of increasing amounts of Hg^{2+} to dyads **5** and **6**, the fluorescence band of the BODIPY unit at 525 nm in dyad **5** and fluorescence band of the BF_2−smaragdyrin unit at 725 nm in dyad **6** gradually increased in intensity, and the their quantum yields increased by 60−70% compared to the respective monomeric fluorophores. These observations indicate that dyads **5** and **6** can be used as fluorescent sensors for Hg^{2+} ion. Thus, in dyads **5** and **6**, the binding of Hg^{2+} at the dithiaporphyrin macrocycle site was measured by following the changes in the fluorescence spectra of the fluorophore unit, which suggests that dyads **5** and **6** can be used as fluorescent sensors.

CONCLUSIONS

In summary, we synthesized and structurally characterized the first stable nonaromatic [20]dithiaporphyrin (2.1.1.1) macrocycles using readily available simple precursors. The macrocycles, which are known as homoporphyrins in the literature, are the first members of expanded porphyrins containing one extra methine carbon at the meso-position compared to [18]porphyrin (1.1.1.1). The unstable homoporphyrins reported in the literature were stabilized by introducing two thiophenes in place of two pyrroles. The macrocycles were found to be highly stable under redox conditions. Furthermore, we showed that the dithiahomoporphyrin macrocycles can be used as an exclusive sensor for Hg^{2+} ion. We synthesized covalently linked homoporphyrin−fluorophore dyads and demonstrated that the dyads can be used as a fluorescent sensor for Hg^{2+} ion. Thus, the synthesis of stable [20]-dithiaporphyrin (2.1.1.1) macrocycles reported here is simple and straightforward, and these macrocycles are now far more accessible for further investigations.

EXPERIMENTAL SECTION

Chemicals. Chemicals such as $BF_3{\cdot}Et_2O$, TFA, *n*-BuLi, $TiCl_4$, and 2,3-dichloro-5,6-dicyano-1,4-benzoquinone (DDQ) were used. All other chemicals used for the synthesis were reagent grade unless otherwise specified. Column chromatography was performed on silica (60−120 mesh) and basic alumina.

Instrumentation. The ^1H, ^{13}C, ^{19}F, and ^{11}B NMR spectra were recorded on 400 and 500 MHz instruments in $CDCl_3$ using tetramethylsilane ($Si(CH_3)_4$) as internal standard for ^1H NMR spectra. ^1H−^1H COSY and NOESY experiments were performed on 400 and 500 MHz instruments. The HR-MS and LR-MS mass spectra were recorded by using the ESI method and a quadrupole analyzer. Cyclic voltammetric (CV) studies were carried out utilizing the three-electrode configuration consisting of glassy carbon (working electrode), platinum wire (auxiliary electrode), and saturated calomel (reference electrode) electrodes. The experiments were performed in dry CH_2Cl_2 using 0.1 M tetrabutylammonium perchlorate as supporting electrolyte. Half-wave potentials were measured using DPV (differential pulse voltammetry) and also calculated manually by taking the average of the cathodic and anodic peak potentials. The quantum yields (Φ) were calculated using rhodamine 6G (Φ = 0.88 in ethanol, λ_{exc} = 488 nm) and H_2TTP (Φ = 0.011 in CH_2Cl_2, λ_{exc} = 450 nm) as references. All Φ are corrected for changes in the refractive index of the solvent. The association constant of the metal complex formed in solution has been estimated by using the standard Benesi−Hildebrand equation, viz.,

$$\frac{1}{I - I_0} = \frac{1}{I_1 - I_0} + \frac{1}{(I_1 - I_0)K_a[M^+]}$$

where I_0 is the intensity of compound **1** before addition of cation, I is the intensity in the presence of M^+, I_1 is intensity upon saturation with M^+, and K_a is the association constant of the complex formed. The solutions of metal chlorates were prepared (1×10^{-3} M) in CH_2Cl_2. The solution containing compounds was placed in a quartz cell (1 cm width), and Hg^{2+} solutions were added in an incremental fashion. Their corresponding UV−vis and fluorescence spectra were recorded at 298 K. In ^1H NMR titration, the spectra were measured on a 400 MHz NMR spectrometer. A solution of **1** in $CDCl_3$ was prepared (5×10^{-3} M), and a 0.4 mL portion of this solution was transferred to a 5 mm NMR tube. Small aliquots of Hg^{2+} were added in an incremental fashion, and their corresponding spectra were recorded.

X-ray Crystallography. Single crystals of suitable size for X-ray diffractometry were selected under a microscope and mounted on the tip of a glass fiber, which was positioned on a copper pin. The X-ray

dx.doi.org/10.1021/jo501724d | J. Org. Chem. 2014, 79, 9603−9612

data for macrocycles **1** and **3** were collected, and graphite-monochromated Mo Kα radiation at 200 K and a $\theta-2\theta$ scan mode were used. The space group for macrocycles **1** and **3** was determined on the basis of systematic absences and intensity statistics, and the structures of macrocycles **1** and **3** were solved by direct methods using SIR92 or SIR97 and refined with SHELXL-97.[14] An empirical absorption correction by multiscans was applied. All non-hydrogen atoms were refined with anisotropic displacement factors. Hydrogen atoms were placed in ideal positions and fixed with relative isotropic displacement parameters. Selected crystallographic data for the macrocycles **1** (CCDC-923462) and **3** (CCDC-1005187) are given in Table 1. These data can be obtained free of charge from The Cambridge Crystallographic Data Centre via www.ccdc.cam.ac.uk/data_request/cif.

2,3-Dithianyl-2-butene ***12***. Activated zinc powder (3.0 g, 46.1 mmol) in THF (80 mL) was placed in a three-necked round-bottom flask, and the vessel was purged with nitrogen gas for 10 min. The mixture was cooled to 0 °C, and $TiCl_4$ (2.52 mL, 23.1 mmol) was added slowly while maintaining the temperature below 0 °C. The suspension was then warmed to room temperature, stirred for 30 min, and refluxed for 3 h. The mixture was again cooled to 0 °C, a solution of 2-acetylthiophene **13** (1.0 mL, 9.2 mmol) in THF (25 mL) was added slowly, and the reaction mixture was refluxed for 12 h, until the starting material was consumed as judged by TLC analysis. The reaction mixture was quenched with 10% aqueous $NaHCO_3$ solution and extracted with ether. The organic layers were collected, dried over anhydrous Na_2SO_4, and concentrated on a rotary evaporator under vacuum. The crude product was purified by chromatography on silica gel using petroleum ether, affording desired product **12** in 72% (1.45 g) yield. R_f (petroleum ether) 0.78; ^{1}H NMR (400 MHz, $CDCl_3$, δ in ppm): 7.15−7.14 (dd, J = 5.0, 5.1 Hz, 2H, α-thiophene), 6.88−6.86 (m, 2H, β-thiophene), 6.78−6.77 (dd, J = 3.6, 3.5 Hz, 2H, β'-thiophene), 2.21 (s, 6H, CH_3). ^{13}C NMR (100 MHz, $CDCl_3$, δ in ppm): 145.8, 145.6, 127.6, 126.72, 126.5, 126.2, 126.1, 125.3, 124.5, 24.1, 22.6.

Compound ***11***. Dried and distilled *n*-hexane (30 mL) was added to a 250 mL three-neck round-bottom flask containing 2,3-dithianyl-2-butene **12** (1.0 g, 4.5 mmol), equipped with a gas inlet tube, a reflux condensor, and a rubber septum. *N*,*N*,*N*′,*N*′-Tetramethylethylenediamine (1.7 mL, 11.4 mmol) and *n*-butyllithium (7 mL, of ca. 15% solution in hexane) were injected into the stirred solution, and the solution was refluxed gently for 1 h. The reaction mixture was then allowed to attain room temperature. An ice-cold solution of *p*-anisaldehyde (1.4 mL, 11.2 mmol) in dry THF (30 mL) was added dropwise to the reaction flask. After the addition was complete, the reaction mixture was allowed to attain room temperature, saturated ammonium chloride solution was added, and the mixture was then extracted with diethyl ether. The organic layers were combined, washed with brine, and dried over anhydrous Na_2SO_4. The crude product was subjected to silica gel column chromatography, and the desired product was eluted with petroleum ether/ethyl acetate (70:30) as a white solid in 65% (1.44 g) yield. R_f (30% petroleum ether/ethyl acetate) 0.39; ^{1}H NMR (400 MHz, $CDCl_3$, δ in ppm): 7.39 (d, J = 6.8 Hz, 4H, Ar), 6.91 (d, J = 6.7 Hz, 4H, Ar), 6.77−6.76 (m, 4H, β-thiophene), 5.98 (s, 2H, CH), 3.81 (s, 6H, OCH_3), 2.42 (br s, 2H, OH), 2.17 (s, 6H, CH_3). ^{13}C NMR (100 MHz, $CDCl_3$, δ in ppm): 159.3, 148.2, 145.8, 135.5, 127.9, 127.8, 125.9, 125.8, 124.5, 124.3, 114.0, 113.8, 72.3, 72.1, 55.4, 24.0, 22.3. HRMS calcd for $C_{28}H_{28}O_4S_2Na$: 515.1321, found 515.1325[M + Na]$^+$. Anal. Calcd for $C_{28}H_{28}O_4S_2$: C, 68.26; H, 5.73. Found: C, 68.20; H, 5.70.

General Synthetic Procedure for Macrocycles 1-4. A sample of 1 equiv of diol **11** (0.2 mmol) and 1 equiv of appropriate *meso*-aryl dipyrromethane **7**-**10** (0.2 mmol) in dry dichloromethane (100 mL) was condensed in the presence of trifluoroacetic acid (0.2 mmol) for 1 h under inert atmosphere at room temperature followed by oxidation with DDQ (0.2 mmol) for an additional 1 h in open air. After removal of the solvent, the crude macrocycle was purified by basic alumina column chromatography using petroleum ether/dichloromethane (1:1) and afforded **1**−**4** as a green lustrous solid in 15−20% yield.

Compound ***1***. Yield 18% (52 mg). R_f (50% petroleum ether/dichloromethane) 0.68; ^{1}H NMR (400 MHz, $CDCl_3$, δ in ppm): 10.80 (bs, 1H, inner NH), 7.23 (d, J = 7.1 Hz, 4H, Ar, type m), 7.21 (d, J = 7.1 Hz, 2H, Ar, type m′), 7.16 (d, J = 7.0 Hz, 2H, Ar, type o′), 6.90−6.88 (m, 4H, β-thiophene type c and d), 6.86 (d, J = 7.0 Hz, 4H, Ar, type o), 6.53 (d, J = 5.0 Hz, 2H, β-pyrrole, type b), 6.31 (d, J = 5.1 Hz, 2H, β-pyrrole type a), 3.82 (s, 6H, OCH_3, type III), 2.38 (s, 3H, tolyl CH_3, type II), 2.12 (s, 6H, ethylene CH_3, type I). ^{13}C NMR (100 MHz, $CDCl_3$, δ in ppm): 159.6, 159.5, 152.1, 150.2, 144.1, 143.6, 136.7, 136.5, 133.5, 133.0, 132.3, 131.8, 131.6, 131.3, 131.1, 131.0, 129.6, 129.0, 128.8, 128.4, 126.9, 124.6, 117.6, 113.7, 113.4, 109.0, 55.4, 22.3, 21.4. UV−vis (in CH_2Cl_2, λ_{max}/nm, log ε) = 412 (5.20) and 720 (4.90). HRMS calcd for $C_{44}H_{37}N_2O_2S_2$: 689.2296, found 689.2305 [M + 1]$^+$. Anal. Calcd for $C_{44}H_{36}N_2O_2S_2$: C, 76.71; H, 5.27; N, 4.07. Found: C, 76.75; H, 5.30; N, 4.09.

Compound ***2***. Yield 16% (45 mg). R_f (50% petroleum ether/dichloromethane) 0.61; ^{1}H NMR (400 MHz, $CDCl_3$, δ in ppm): 10.79 (bs, 1H, inner NH), 7.24 (d, J = 8.6 Hz, 2H, Ar, type m′), 7.23 (d, J = 8.8 Hz, 4H, Ar, type m), 6.89 (d, J = 8.9 Hz, 2H, Ar, type o′), 6.87 (d, J = 8.8 Hz, 4H, Ar, type o), 6.86−6.85 (m, 4H, β thiophene, type c and d), 6.53 (d, J = 5.1 Hz, 2H, β-pyrrole, type b), 6.30 (d, J = 5.1 Hz, 2H, β-pyrrole, type a), 3.85 (s, 3H, OCH_3, type II), 3.83 (s, 6H, OCH_3, type III), 2.12 (s, 6H, ethylene CH_3, type I). ^{13}C NMR (100 MHz, $CDCl_3$, δ in ppm): 159.7, 159.2, 152.1, 150.5, 143.7, 143.2, 136.7, 135.5, 134.5, 133.1, 132.1, 131.8, 131.6, 131.34, 130.2, 129.6, 129.0, 128.8, 128.6, 126.5, 124.6, 117.6, 113.7, 113.4, 55.2, 55.0, 22.2. UV−vis (in CH_2Cl_2, λ_{max}/nm, log ε) = 410 (5.36) and 724 (4.83). HRMS calcd for $C_{44}H_{37}N_2O_3S_2$: 705.2246; found 705.2223 [M + 1]$^+$. Anal. Calcd for $C_{44}H_{36}N_2O_3S_2$: C, 74.97; H, 5.15; N, 3.97. Found: C, 74.95; H, 5.11; N, 3.94.

Compound ***3***. Yield 19% (44 mg). R_f (50% petroleum ether/dichloromethane) 0.74; ^{1}H NMR (400 MHz, $CDCl_3$, δ in ppm): 10.77 (bs, 1H, inner NH), 7.69 (d, J = 8.2 Hz, 2H, Ar, type o′), 7.23 (d, J = 8.7 Hz, 4H, Ar, type m), 7.09 (d, J = 8.3 Hz, 2H, Ar, type m′), 6.91−6.88 (m, 4H, β-thiophene, type c and d), 6.86 (d, J = 8.7 Hz, 4H, Ar, type o), 6.56 (d, J = 5.0 Hz, 2H, β-pyrrole, type b), 6.27 (d, J = 5.1 Hz, 2H, β-pyrrole, type a),3.83 (s, 6H, OCH_3 type III), 2.13 (s, 6H, ethylene CH_3, type I). ^{13}C NMR (100 MHz, $CDCl_3$, δ in ppm): 159.6, 159.1, 152.3, 150.0, 143.9, 139.5, 137.5, 137.3, 134.0, 133.4, 133.1, 132.4, 132.2, 131.5, 131.1, 129.1, 126.3, 125.3, 113.7, 113.4, 55.4, 22.3. UV−vis (in CH_2Cl_2, λ_{max}/nm, log ε) = 412 (5.26), 722 (4.86). HRMS calcd for $C_{43}H_{34}N_2O_2S_2I$: 801.1106; found 801.1107 [M + 1]$^+$. Anal. Calcd for $C_{43}H_{33}N_2O_2S_2I$: C, 64.50; H, 4.15; N, 3.50. Found: C, 64.58; H, 4.22; N, 3.56.

Compound ***4***. Yield 15% (40 mg). R_f (50% petroleum ether/dichloromethane) 0.53; ^{1}H NMR (400 MHz, $CDCl_3$, δ in ppm): 10.86 (bs, 1H, inner NH), 8.24 (d, J = 6.9 Hz, 2H, Ar, type o′), 7.53 (d, J = 6.9 Hz, 2H, Ar, type m′), 7.24 (d, J = 7.0 Hz, 4H, Ar, type m), 6.93−6.91 (m, 4H, β-thiophene, type c and d), 6.87 (d, J = 6.7 Hz, 4H, Ar, type o), 6.63 (d, J = 5.1 Hz, 2H, β-pyrrole, type b), 6.27 (d, J = 5.1 Hz, 2H, β-pyrrole, type a),3.83 (s, 6H, OCH_3, type III), 2.14 (s, 6H, ethylene CH_3, type I). ^{13}C NMR (100 MHz, $CDCl_3$, δ in ppm): 159.8, 158.7, 152.6, 149.6, 146.7, 143.7, 133.2, 132.8, 132.5, 131.9, 131.2, 128.4, 126.4, 123.5, 113.5, 55.5, 22.3. UV−vis (in CH_2Cl_2, λ_{max}/nm, log ε) = 406 (5.17), 716 (4.94). HRMS calcd for $C_{43}H_{33}N_3O_4S_2$: 719.1913; found 719.1945 [M]$^+$. Anal. Calcd for $C_{43}H_{33}N_3O_4S_2$: C, 71.74; H, 4.62; N, 5.84. Found: C, 71.70; H, 4.57; N, 5.79.

General Procedure for Covalently Linked Dyads ***5*** *and* ***6***. A solution of 1 equiv of ethynyl-containing chromophores **14** and **15** (0.025 mmol) and 1 equiv of iodo-functionalized macrocycle **3** (15 mg, 0.02 mmol) in dry toluene/triethyleamine (3:1) was purged with nitrogen for 15 min. The coupling was initiated by adding $AsPh_3$ (1.5 mg, 0.002 mmol) followed by $Pd_2(dba)_3$ (2 mg, 0.002 mmol), and the reaction mixture was stirred at 40 °C for 5 h. TLC analysis indicated the appearance of new spot apart from the small amount of corresponding unreacted monomers. The crude reaction mixture was purified by basic alumina chromatography using petroleum ether/dichloromethane as eluent. The excess $AsPh_3$ and small amounts of unreacted monomers were removed first, and the homoporphyrin−

dx.doi.org/10.1021/jo501724d | J. Org. Chem. 2014, 79, 9603−9612

chromophore dyads **5** and **6** were then collected using petroleum ether/dichloromethane.

Compound ***5***. Yield 61% (11 mg); R_f (60% petroleum ether/dichloromethane) 0.32; ^{1}H NMR (400 MHz, $CDCl_3$, δ in ppm): 10.85 (bs, 1H, inner NH), 7.96 (s, 2H, py), 7.70 (d, J = 4.9 Hz, 2H, Py), 7.58 (d, J = 8.1 Hz, 4H, Ar), 7.37 (d, J = 4.8 Hz, 2H, Py), 7.24 (d, J = 8.1 Hz, 4H, Ar), 6.96 (d, J = 8.2 Hz, 2H, Py), 6.93−6.91 (m, 4H, Ar), 6.86 (d, J = 4.9 Hz, 4H, thiophene), 6.59−6.57 (m, 4H, Ar + Py), 6.33 (d, J = 5.0 Hz, 2H, Py), 3.84 (s, 6H, OCH_3), 2.15 (s, 6H, CH_3). ^{11}B NMR (96.3 MHz, $CDCl_3$, δ in ppm): 0.54 (t, J_{B-F} = 28.99 Hz). ^{19}F NMR (282.2 MHz, $CDCl_3$, δ in ppm): −145.03 (q, J_{B-F} = 56.4 Hz). ^{13}C NMR (100 MHz, $CDCl_3$, δ in ppm): 157.0, 152.1, 147.9, 147.3, 142.7, 141.2, 140.9, 140.6, 140.2, 139.6, 138.2, 136.3, 136.0, 135.8, 133.7, 133.5, 132.7, 132.5, 131.6, 131.3, 131.0, 130.9, 130.6, 129.5, 128.7, 121.9, 114.3, 106.2, 105.9, 105.3, 58.9, 55.6. UV−vis (in CH_2Cl_2, λ_{max}/nm, log ε) = 416 (5.31), 504 (5.24) 718 (4.78). λ_{em} (nm) = 527. HRMS calcd for $C_{60}H_{44}BF_2N_4O_2S_2$: 965.2971; found 965.2986 $[M + 1]^+$.

Compound ***6***. Yield 60% (15 mg); R_f (60% petroleum ether/dichloromethane) 0.45; ^{1}H NMR (400 MHz, $CDCl_3$, δ in ppm): 10.94 (bs, 1H, inner NH), 10.32 (d, J = 4.5 Hz, 2H, Py), 10.23−1022 (m, 2H, Py), 9.61 (d, J = 4.4 Hz, 2H, Py), 9.47 (s, 2H, furan), 9.00−8.99 (m, 2H, Py), 8.62 (d, J = 8.1 Hz, 2H, Ar), 8.30 (d, J = 8.0 Hz, 4H, Ar), 8.16 (d, J = 8.1 Hz, 2H, Ar), 7.75 (d, J = 8.1 Hz, 2H, Ar), 7.73 (d, J = 8.0 Hz, 4H, Ar), 7.46 (d, J = 8.1 Hz, 2H, Ar), 7.31 (d, J = 8.0 Hz, 2H, Ar), 7.27 (d, J = 8.0 Hz, 4H, Ar), 6.94 (d, J = 5.0 Hz, 4H, thiophene), 6.89 (d, J = 8.1 Hz, 2H, Ar), 6.64 (d, J = 5.0 Hz, 2H, Py), 6.42 (d, J = 5.0 Hz, 2H, Py), 3.85 (s, 6H, OCH_3), 2.79 (s, 6H, CH_3), 2.15 (s, 6H, CH_3), −3.82 (bs, 2H, inner NH). ^{11}B NMR (96.3 MHz, $CDCl_3$, δ in ppm): −13.62 (bs), ^{19}F NMR (282.2 MHz, $CDCl_3$, δ in ppm): −149.39 (bs). ^{13}C NMR (100 MHz, $CDCl_3$, δ in ppm): 162.4, 149.9, 148.3, 147.5, 146.9, 143.9, 139.7, 138.0, 135.5, 134.4, 134.0, 133.7, 132.8, 132.1, 131.6, 130.7, 129.5, 128.4, 126.9, 126.5, 125.8, 125.1, 124.5, 123.8, 122.2, 121.8, 121.3, 120.8, 120.3, 119.4, 118.7, 115.6, 114.4, 114.1, 113.3, 107.2, 55.7, 53.6. UV−vis (in CH_2Cl_2, λ_{max}/nm, log ε) = 423 (4.90), 450 (5.54), 474 (5.13), 590 (4.29), 650 (4.46), 710 (4.81). λ_{em} (nm) = 722. HRMS calcd for $C_{88}H_{64}BF_2N_6O_3S_2$: 1365.4550; found 1365.4595 $[M + 1]^+$.

■ ASSOCIATED CONTENT

Ⓢ Supporting Information

NMR spectra of the compounds and absorption, crystallographic, and computational data. This material is available free of charge via the Internet at http://pubs.acs.org.

■ AUTHOR INFORMATION

Corresponding Authors

*E-mail: wzlee@ntnu.edu.tw.

*E-mail: ravikanth@chem.iitb.ac.in.

Notes

The authors declare no competing financial interest.

■ ACKNOWLEDGMENTS

M.R. acknowledges the financial support provided by DST, Govt. of India. E.G. thanks UGC for a senior research fellowship. We also thank Dr. Avijit Ghosh for his help in plotting X-ray structures.

■ REFERENCES

(1) *The Porphyrin Handbook*; Kadish, K. M.; Smith, K. M.; Guilard, R., Eds.; Academic Press: San Diego, 2000; Vol. *6*.

(2) (a) Jasat, A.; Dolphin, D. *Chem. Rev.* **1997**, *97*, 2267−2340. (b) Sessler, J. L.; Weghorn, S. J. *Organic Chemistry Series*; Pergamon: New York, 1997; Vol. *15*. (c) Sessler, J. L.; Siedel, D. *Angew. Chem., Int. Ed.* **2003**, *42*, 5134−5175. (d) Chandrashekar, T. K.; Venkatraman, S. *Acc. Chem. Res.* **2003**, *36*, 676−691. (e) Saito, S.; Osuka, A. *Angew. Chem., Int. Ed.* **2011**, *50*, 4342−4373.

(3) Grigg, R. *J. Chem. Soc., Chem. Commun.* **1967**, 1238−1239.

(4) (a) Callot, H. J.; Tschamber, T. *Tetrahedron Lett.* **1974**, 3155. (b) Callot, H. J.; Tschamber, T. *J. Am. Chem. Soc.* **1975**, *97*, 6175. (c) Callot, H. J.; Tschamber, T. *J. Org. Chem.* **1977**, *42*, 1567. (d) Callot, H. J.; Schaeffer, E. *Tetrahedron* **1978**, *34*, 2295. (e) Callot, H. J.; Tschamber, T.; Schaeffer, E. *Tetrahedron Lett.* **1975**, 2919. (f) Louati, A.; Schaeffer, E.; Callot, H. J.; Gross, M. *Nouv. J. Chim.* **1979**, *3*, 191.

(5) Osuka, A.; Saito, S. *Chem. Commun.* **2011**, *47*, 4330−4339. (b) Lim, J. M.; Shin, J. Y.; Tanaka, Y.; Saito, S.; Osuka, A.; Kim, D. *J. Am. Chem. Soc.* **2010**, *132*, 3104−3114. (c) Tanaka, Y.; Saito, S.; Mori, S.; Aratani, N.; Shinokubo, H.; Shibata, N.; Higuchi, Y.; Yoon, Z. S.; Kim, K. S.; Noh, S. B.; Park, J. K.; Kim, D.; Osuka, A. *Angew. Chem., Int. Ed.* **2008**, *47*, 681−684.

(6) (a) Sessler, J. L.; Weghorn, S. J.; Hiseada, Y.; Lynch, V. *Chem.—Eur. J.* **1995**, *1*, 56−66. (b) Krivokapic, A.; Cowley, A. R.; Anderson, H. L. *J. Org. Chem.* **2003**, *68*, 1089−1096. (c) Hannah, S.; Seidel, D.; Sessler, J. L.; Lynch, V. *Inorg. Chim. Acta* **2001**, *317*, 211−217. (d) Sessler, J. L.; Seidel, D.; Vivan, A. E.; Lynch, V.; Scott, B. L.; Keogh, D. W. *Angew. Chem., Int. Ed.* **2001**, *40*, 591−594. (e) Yoon, M.-C.; Cho, S.; Suzuki, M.; Osuka, A.; Kim, D. *J. Am. Chem. Soc.* **2009**, *131*, 7360−7367. (f) Rath, H.; Aratani, N.; Lim, J. M.; Lee, J. S.; Kim, D.; Shinokubo, H.; Osuka, A. *Chem. Commun.* **2009**, 3762−3764. (g) Sankar, J.; Mori, S.; Saito, S.; Rath, H.; Suzuki, M.; Inokuma, Y.; Shinokubo, H.; Kim, K. S.; Yoon, Z. S.; Shin, J.-Y.; Lim, J. M.; Matsuzuki, Y.; Matsushita, O.; Muranaka, A.; Kobayashi, N.; Kim, D.; Osuka, A. *J. Am. Chem. Soc.* **2008**, *130*, 13568−13579. (h) Sessler, J. L.; Seidel, D.; Lynch, V. *J. Am. Chem. Soc.* **1999**, *121*, 11257−11258. (i) Shimizu, S.; Aratani, N.; Osuka, A. *Chem.—Eur. J.* **2006**, *12*, 4909−4918. (j) Gopalakrishna, T. Y.; Reddy, J. S.; Anand, V. G. *Angew. Chem., Int. Ed.* **2013**, *52*, 1763−1767. (k) Alonso, M.; Geerlings, P.; Proft, F. D. *Chem.—Eur. J.* **2013**, *19*, 1617−1628. (l) Sprutta, N.; Latos-Grażyński, L. *Chem.—Eur. J.* **2001**, *7*, 5099−5112. (m) Sessler, J. L.; Seidel, D.; Gebauer, A.; Lynch, V.; Abboud, K. A. J. *Heterocycl. Chem.* **2001**, *38*, 1419−1424. (n) Sessler, J. L.; Weghorn, S. J.; Lynch, V.; Johnson, M. R. *Angew. Chem., Int. Ed. Engl.* **1994**, *33*, 1509−1512. (o) Setsune, J.-I.; Katakami, Y.; Iizuna, N. *J. Am. Chem. Soc.* **1999**, *121*, 8957−8958. (p) Setsune, J.-I.; Maeda, S. *J. Am. Chem. Soc.* **2000**, *122*, 12405−12406.

(7) Chang, Y.; Chen, H.; Zhou, Z.; Zhang, Y.; Schütt, C.; Herges, R.; Shen, Z. *Angew. Chem., Int. Ed.* **2012**, *51*, 12801−12805.

(8) Latos-Grażyński, L. *The Porphyrin Handbook*; Kadish, K. M.; Smith, K. M.; Guilard, R., Eds.; Academic Press: San Diego, 2000; Vol. *2*, pp 361−416.

(9) Lee, C.-H; Lindsey, J. S. *Tetrahedron* **1994**, *50*, 11427−11440.

(10) (a) Toullec, P.; Ricard, L.; Mathey, F. *Organometallics* **2002**, *21*, 2635−2638. (b) Duan, X.-F.; Zeng, J.; Zhang, Z.-B.; Zi, G.-F. *J. Org. Chem.* **2007**, *72*, 10283−10286.

(11) Schleyer, P. v. R.; Maerker, C.; Dransfeld, A.; Jiao, H.; Hommes, N. J. R. v. E. *J. Am. Chem. Soc.* **1996**, *118*, 6317−6318.

(12) Frisch, M. J. et al. *Gaussian 03 (Revision C.02)*; Gaussian, Inc., Wallingford, CT, 2004. For the full reference, see Supporting Information.

(13) Wagner, R. W.; Johnson, T. E.; Li, F.; Lindsey, J. S. *J. Org. Chem.* **1995**, *60*, 5266−5273.

(14) Sheldrick, G. M. *Acta Crystallogr., Sect. A: Found. Crystallogr.* **2008**, *A64*, 112. *Program for Crystal Structure Solution and Refinement*; University of Goettingen, Goettingen, Germany, 1997.